OPEN ACCESS
IOP Publishing | Astro Ltd
Laser Physics Letters
Laser Phys. Lett. **19** (2022) 056202 (4pp)
https://doi.org/10.1088/1612-202X/ac61d4

Letter

Angstrom-precise fabrication of surface nanoscale axial photonics (SNAP) microresonators with a flame

Misha Sumetsky* **and Victor Vassiliev**

Aston Institute of Photonic Technologies, Aston University, Birmingham, United Kingdom, B4 7ET

E-mail: m.sumetsky@aston.ac.uk

Received 21 March 2022
Accepted for publication 23 March 2022
Published 7 April 2022

Abstract

We demonstrate the fabrication of surface nanoscale axial photonics bottle microresonators with angstrom precision using a flame. We observe strongly unscalable behavior of the whispering gallery mode cutoff wavelengths with different radial quantum numbers along the fibre length.

Keywords: optical microresonators, whispering gallery modes, nanoscale, cutoff wavelength

(Some figures may appear in colour only in the online journal)

1. Introduction

Melting a silica fibre is a common way to fabricate whispering gallery mode (WGM) optical microresonators. Melting can be performed in a flame, in a CO_2 laser beam, in an arc discharge, and in an electric heater (see [1–4] and references therein). The Q-factor of microresonators created by melting can achieve dramatically high values up to 10^{10} [1]. However, the melting process is not accurately reproducible and, usually, has the precision of a few microns [3]. This precision can be further improved by post-processing, e.g. by HF etching [5, 6].

Even with the same shape, WGM microresonators fabricated from the same material using different methods can have different spectral characteristics. For comparison, the etching process does not affect the bulk material refractive index. Alternatively, CO_2 laser and flame heating do introduce the refractive index variation, though differently: the laser beam heats the optical material internally, while the flame heats it externally [7, 8]. As a result, the distribution of refractive index and, hence, WGMs in microresonators fabricated with these three approaches can be different.

In this letter, we use a flame to locally anneal the optical fibre. We show that annealing with flame can achieve dramatically better precision than melting. This is primarily explained by the fact that annealing, which releases the frozen-in tension introduced during the fibre drawing, causes much smaller deformation of the fibre material than melting. As a result, the effective radius of the fibre experiences nanoscale variation (summarizing its physical radius and refractive index variations), which produces an exceptionally shallow bottle microresonator called a surface nanoscale axial photonics (SNAP) microresonator (SMR) [9, 10]. Previously, several approaches for fabrication of SMRs have been developed based on CO_2 laser annealing [9, 10], femtosecond laser inscription [11], bending [12], slow cooking [13], and etching [6]. In this report, we develop the flame-based approach for the fabrication of SMRs and demonstrate its angstrom precision. In contrast to SMRs fabricated by annealing with a CO_2 laser [9, 10], we observe strongly unscalable behaviour of WGM cutoff wavelengths with different radial quantum numbers along the fibre length important for a range of applications.

* Author to whom any correspondence should be addressed.

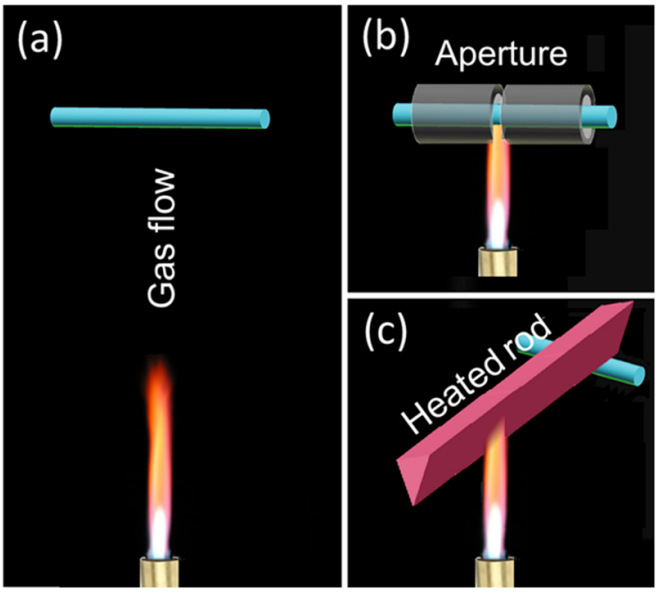

Figure 1. Fabrication of SNAP microresonators using (a) flame heated gas flow, (b) apertured flame, and (c) indirect flame heating.

2. Fabrication of SMRs

The schematics of devices used in our experiments are shown in figure 1. In all cases, we used a torch which was fed with the butane/propane mixture. The fibre segment was oriented horizontally, and the flame was oriented vertically. In the setup illustrated in figure 1(a), an optical fibre was placed at the 10 cm distance from the visible flame. In this case, the fibre was annealed by a localized flow of gas, which was sufficiently hot to induce the required permanent effective radius variation of the fibre. In order to decrease the microresonator length along the fibre axis, we used an aperture, which was fabricated of sapphire tubes with outer diameter 3 mm and inner diameter 1.2 mm illustrated in figure 1(b). The aperture size in this experiment was 2 mm. In the approach illustrated in figure 1(c), an optical fibre was annealed indirectly [14] using a metal rod heated by the flame. This approach allowed us to significantly suppress the effects of gas flow and stabilize the heating temperature. To fabricate an SMR, the fibre was translated with the speed $\sim$15–20 mm s^{-1}. In the cases shown in figures 1(a)–(c), the fibre was translated with a constant speed normally to its axial direction and flame direction. Consequently, the fibre was annealed during fractions of a second time when it was passing the hot region. In the case shown in figure 1(c), the fibre was translated normally to its axis and parallelly to the flame direction first towards to and then immediately backwards from the heated rod. The annealing time was approximately the same.

3. Characterization of SMRs

We characterized the spectra of fabricated SMRs by scanning them with the micron diameter waist (microfibre) of a biconically tapered optical fibre connected to an optical spectrum analyzer (OSA), Luna 5000. The microfibre was oriented normally to the characterized fibre segments. In the process of translation along the fibre axis, the microfibre periodically touched it at points where the amplitude of resonant transmission through SMRs was measured [9, 10]. Figure 2 shows the results of our experiments using three approaches illustrated in figure 1. This figure shows the spectrograms of fabricated SMRs, i.e. the two-dimensional plots of the transmission power spectrum $P(z,\lambda)$ as a function of the microfibre position along the SMR axis z and wavelength λ. The lines in all spectrograms, indicate the WGM cutoff wavelengths which vary along the fibre axis and serve as envelops for the spectrum of fabricated SMFs. Due to the large mm-scale length of introduced SMFs, their spectra are not resolved with our OSA resolution 1.3 pm except for shorter SMRs in figures 2(b) and (d). In our experiments we used the standard 125 μm fibre to obtain the results shown in figures 2(a), (b) and (e), and 40 μm fibre for the results shown in figures 2(c) and (d). Figures 2(a)–(c) show the spectrograms of SMRs fabricated by distance annealing illustrated in figure 1(a). Series of SMRs in figures 2(a) and (b) correspond to the undersaturated case when the frozen-in tension is not fully released. The SMR profiles in figure 2(b) are oversaturated. In the latter case, the heating temperature exceeds the annealing temperature, the fibre start softening, and fabrication reproducibility worsens. Figure 2(c) shows the saturated flat SMR profile [9]. Using the sapphire tube aperture illustrated in figure 1(b), allowed us to fabricate shorter SMRs which spectrogram is shown in figure 2(d). Comparison of the SMR spectrograms with the profile of unprocessed fibre, allowed us to conclude that these SMRs were fabricated with the precision of 5 pm in wavelength and 0.7 angstrom in the effective fibre radius variation. Thus, the angstrom fabrication precision of SMRs with a flame has been achieved. Finally, we fabricated SMRs by indirect heating with a setup illustrated in figure 1(c). In this case, the spectrogram of SMRs shown in figure 2(e) demonstrated the completely unscalable axial profiles of cutoff wavelength variations corresponding to

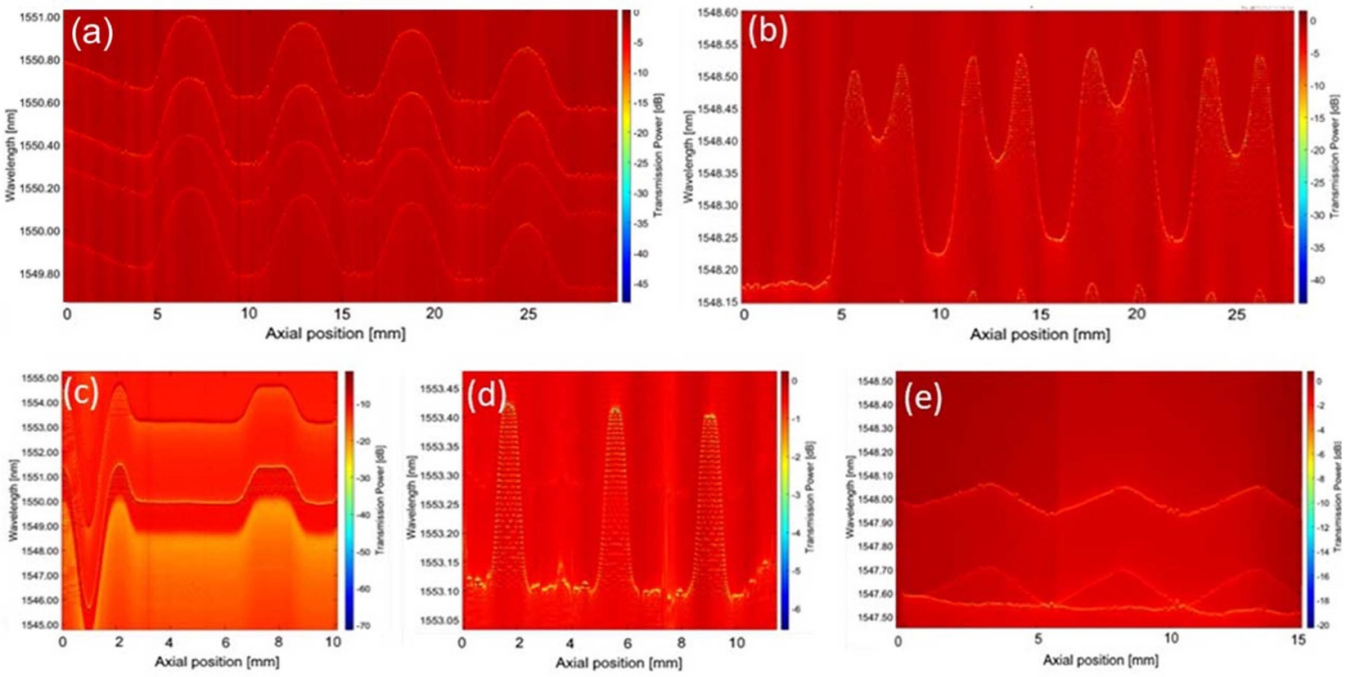

Figure 2. Spectrograms of SMRs fabricated with methods illustrated in figure 1. (a)–(c) Distant gas flow heating. (d) Apertured flame heating. (e) Indirect flame heating.

different radial quantum numbers. We observed the introduction of the triangular-shaped cutoff wavelength variation for one series of WGMs simultaneously with the remaining axial independent, i.e. unaffected by the annealing process, cutoff wavelength for other series. We attribute this effect to the qualitatively different spatial (along the fibre radial direction) and time dependencies of heating power induced by a flame in the case shown in figure 2(e) as compared to that in figure 2(a) and also to internal heating by a CO_2 laser beam [9, 10], where so strong unscalable behaviour of WGM cutoff wavelengths has not been observed.

4. Discussion

We demonstrated that using a simple flame torch it is possible to fabricate optical microresonators with angstrom precision. The developed approach allows us to fabricate SMRs having smooth elongated profiles. A more detailed study of the SMRs with spectrogram shown in figure 2(a) (not included here) showed that the tops of several fabricated SMRs have a precise parabolic shape important for the fabrication of miniature delay lines [15] and frequency comb generators [16]. Fabrication of such SMRs using approaches previously developed in the SNAP technology [9–13] was challenging. In addition, the unscalable behaviour of cutoff wavelength (figure 2(e)) can be used for the controlled all-optical manipulation of slow whispering gallery light pulses when the propagation of strong control and weak controlled pulses are governed by different axial cutoff wavelength variations [17, 18]. Future improvement of our approach will include experimental development and optimization of setups illustrated in figure 1 and modelling of the transient heating processes induced by a flame.

Acknowledgments

The authors acknowledge funding from Engineering and Physical Sciences Research Council (EPSRC) under Grant EP/P006183/1 and from Horizon 2020 under MSCA-ITN-EID Grant 814147.

References

[1] Gorodetsky M L, Savchenkov A A and Ilchenko V S 1996 *Opt. Lett.* **21** 453–5
[2] Knight J C, Cheung G, Jacques F and Birks T A 1997 *Opt. Lett.* **22** 1129–31
[3] Pollinger M, OShea D, Warken F and Rauschenbeutel A 2009 *Phys. Rev. Lett.* **103** 053901
[4] Murugan G S, Wilkinson J S and Zervas M N 2009 *Opt. Express* **17** 11916–25
[5] Lee H, Chen T, Li J, Yang K Y, Jeon S, Painter O and Vahala K J 2012 *Nat. Photon.* **6** 369–73
[6] Toropov N, Zaki S, Vartanyan T and Sumetsky M 2021 *Opt. Lett.* **46** 1784–7
[7] Kakarantzas G, Dimmick T E, Birks T A, Le Roux R and Russell P S J 2001 *Opt. Lett.* **26** 1137–9
[8] Sumetsky M, Dulashko Y and Windeler R S 2010 *Opt. Lett.* **35** 898–900
[9] Sumetsky M, DiGiovanni D J, Dulashko Y, Fini J M, Liu X, Monberg E M and Taunay T F 2011 *Opt. Lett.* **36** 4824–6
[10] Sumetsky M 2013 *Nanophotonics* **2** 393
[11] Yu Q, Zhang Z and Shu X 2021 *Opt. Lett.* **46** 1005–8
[12] Bochek D, Toropov N, Vatnik I, Churkin D and Sumetsky M 2019 *Opt. Lett.* **44** 3218–21

[13] Gardosi G, Mangan B J, Puc G S and Sumetsky M 2021 *ACS Photonics* **8** 436–42
[14] Tong L, Gattass R R, Ashcom J B, He S, Lou J, Shen M, Maxwell I and Mazur E 2003 *Nature* **426** 816–9
[15] Sumetsky M 2013 *Phys. Rev. Lett.* **111** 163901
[16] Suchkov S V, Sumetsky M and Sukhorukov A A 2017 *Opt. Lett.* **42** 2149–52
[17] Sumetsky M 2016 *Sci. Rep.* **5** 18569
[18] Crespo-Ballesteros M and Sumetsky M 2021 *Phys. Rev. Lett.* **126** 15390